The Effects of two Parameters on idealized Convective Boundary Layer Entrainment
M.Sc. Defense

Niamh Chaparro

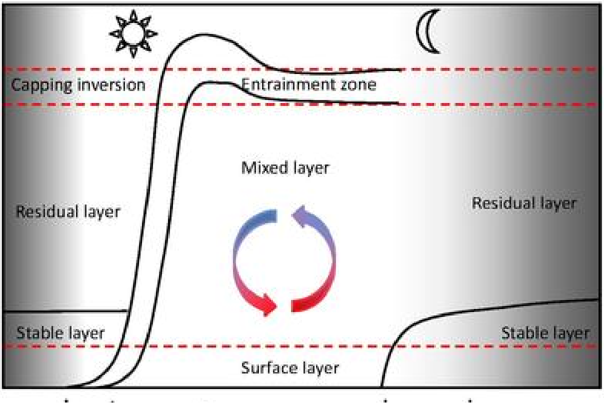

Figure 1: Representation of the time evolution of the convective boundary layer adapted from Stull 1988.

Knowledge of the convective boundary layer (CBL) and its entrainment zone (EZ) is important because:

- CBL height is needed to calculate CBL concentrations
- knowledge of EZ depth and lifting condensation level enables cloud cover prediction
- parameterizations for both are required in global circulation models (GCMs)

Three types of CBL entrainment Studies:

1. measurement based
2. numerical models that solve the Navier Stokes Equations: large eddy simulation (LES), direct numerical simulation (DNS)
3. bulk models based on average quantities and simplified profiles

There is ongoing discussion about:

- the critical discrete resolution for capturing entrainment in numerical models
- the multitude of definitions of CBL height and EZ boundaries
- the form of the relationships of CBL growth (w_e entrainment rate) and EZ depth (Δh) to convective Richardson number (Ri defined later)

I modelled a dry, idealized CBL w/out large scale winds and:

- applied optimal discrete resolution ($\Delta x = 25m$, $\Delta y = 25m$ and $\Delta z = 5m$)
  (Peter P. Sullivan and Edward G. Patton 2011)

- defined CBL height and EZ limits based on the average θ profile

- investigated the resulting relationships of w_e and Δh to Ri:

I used LES, System for Atmospheric Modelling (SAM) which:

- solves the Anelastic equations of motion on an Arakawa c grid
- prognoses Liquid/Ice static energy (h_l)
- uses first order Smagorinksi closure
- advects scalars using a three dimensional positive definite scheme

Table 1: Table of 10-ensemble runs in terms of the two external parameters: surface heat flux ($\overline{w'\theta'_s}$) and initial Lapse Rate γ. These legends will be used in plots throughout.

$\overline{w'\theta'_s}$ / γ	10 (K/Km)	5 (K/Km)	2.5 (K/Km)
150 (W/m2)	▼ 150/10	● 150/5[1]	
100 (W/m2)	▼ 100/10	● 100/5	
60 (W/m2)	▼ 60/10	● 60/5	★ 60/2.5

[1]Incomplete Run: EZ exceeded high resolution vertical grid after 7 hours

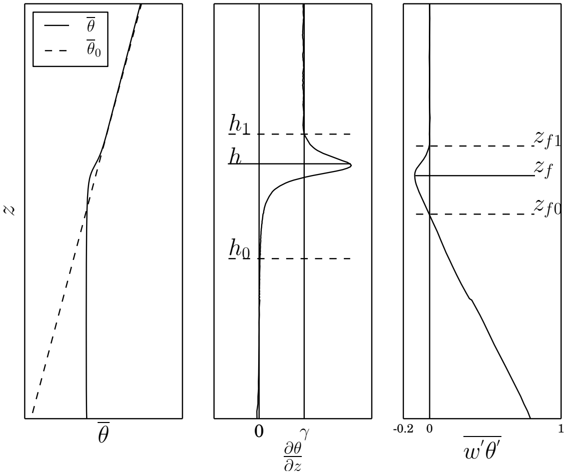

Figure 2: Height definitions based on the average vertical profiles: θ_0 is the initial potential temperature. $\Delta h = h_1 - h_0$

Table 2: Definitions based on the vertical $\overline{\theta}$ profile in Figure 2.

CBL Height	ML $\overline{\theta}$ ($\overline{\theta}_{ML}$)	Deardorff Velocity Scale (w^*)	θ Jump ($\Delta\theta$)	Richardson Number (Ri)
h	$\frac{1}{h}\int_0^h \overline{\theta}(z)dz$	$\left(\frac{gh}{\overline{\theta}}(\overline{w'\theta'})_s\right)^{\frac{1}{3}}$	$\overline{\theta}(h_1) - \overline{\theta}(h_0)$	$\frac{\frac{g}{\overline{\theta}_{ML}}\Delta\theta h}{w^{*2}}$

Figure 3: Horizontal slice of potential temperature (θ): darker shading represents θ close to the mixed layer average ($\overline{\theta}_{ML}$) and lighter represents warmer θ.

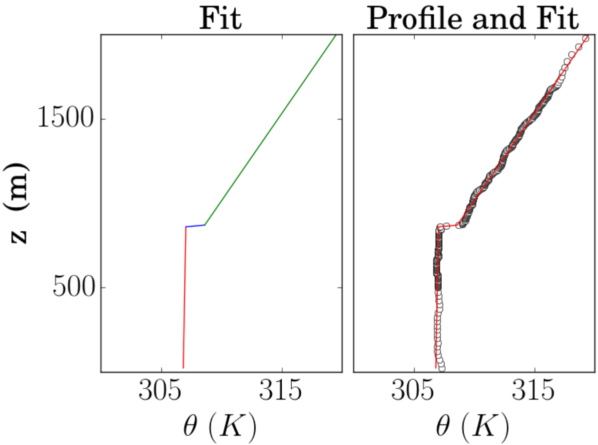

Figure 4: Local θ profile at a single horizontal point where height is relatively high, at 5 simulated hours (right). Tri-linear fit to the local θ profile (left) with a line for each of the 3 layers: mixed layer (ML), EZ and free atmosphere (FA).

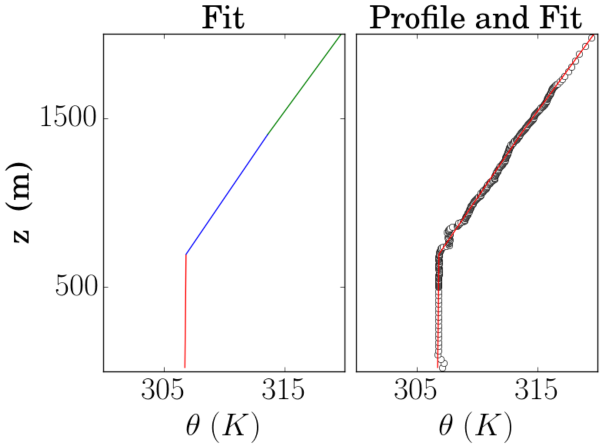

Figure 5: As in previous slide but at a point where height is relatively low.

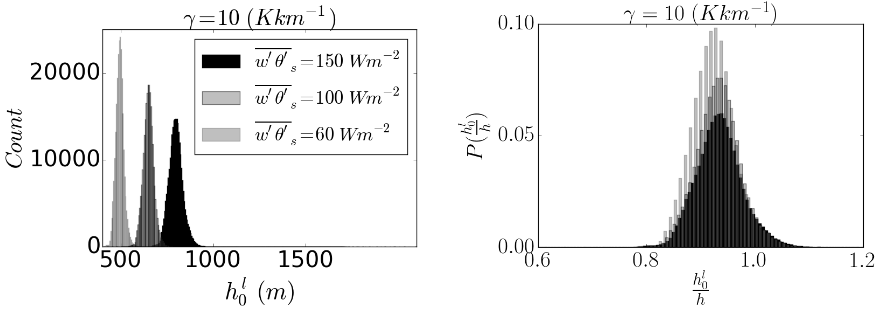

Figure 6: Distribution of local ML heights (left). PDF of local ML heights scaled by h (right). h is the CBL height based on maximum average vertical θ gradient.

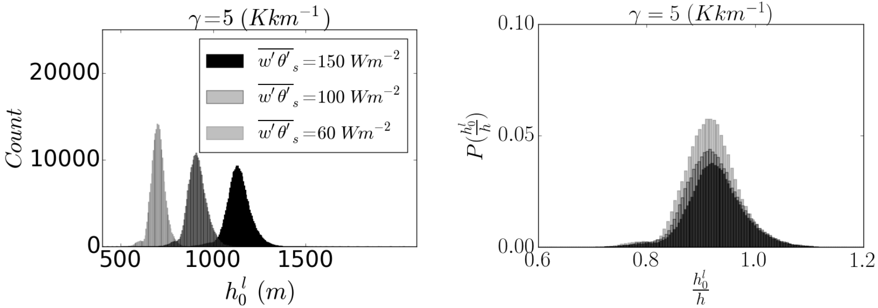

Figure 7: As previous slide but with lower γ

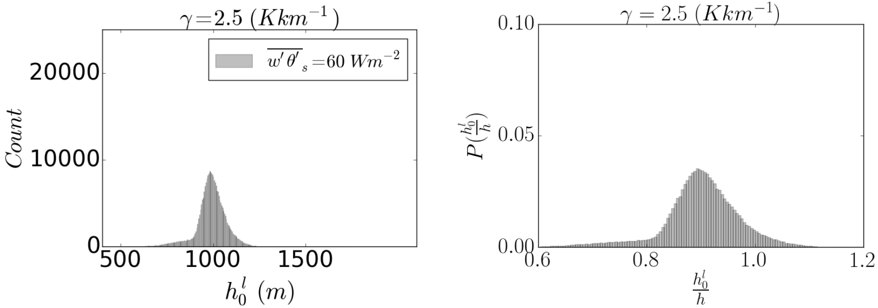

Figure 8: As previous slide but with lower γ

Conclusion:

- **The scaled lowest local CBL heights increase with increased stability**

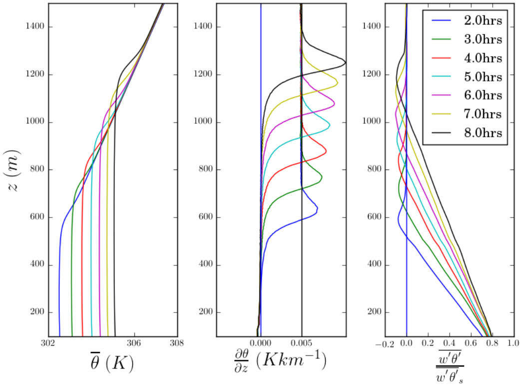

Figure 9: Evolution of (left) ensemble and horizontally averaged θ, (middle) its vertical gradient ($\frac{\partial\overline{\theta}}{\partial z}$) and (right) vertical heat flux ($\overline{w'\theta'}$)

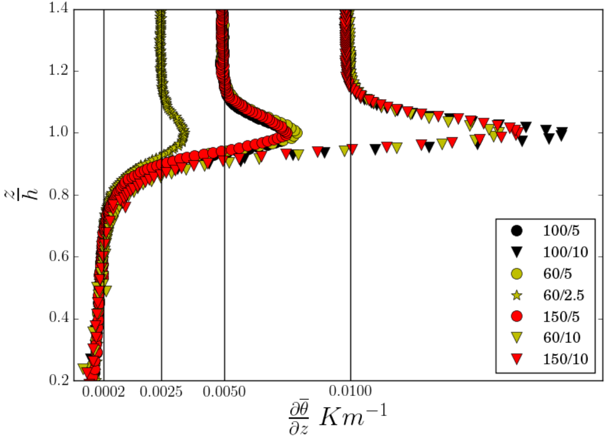

Figure 10: Threshold value for defining the lower EZ boundary based on $\frac{\partial\overline{\theta}}{\partial z}$

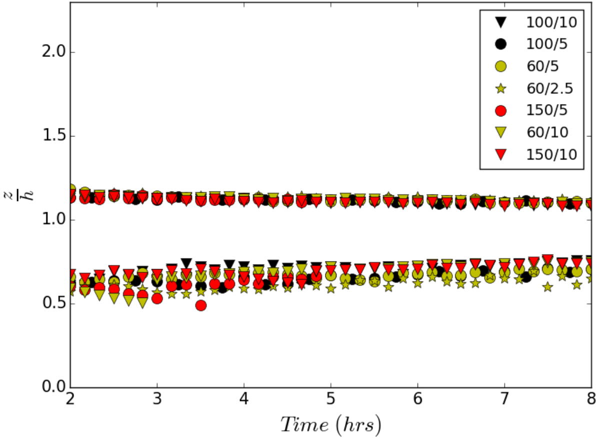

Figure 11: Scaled upper and lower EZ boundaries defined based on $\frac{\partial \bar{\theta}}{\partial z}$

Conclusion:

- **The scaled lower EZ boundary increases with increased Ri**

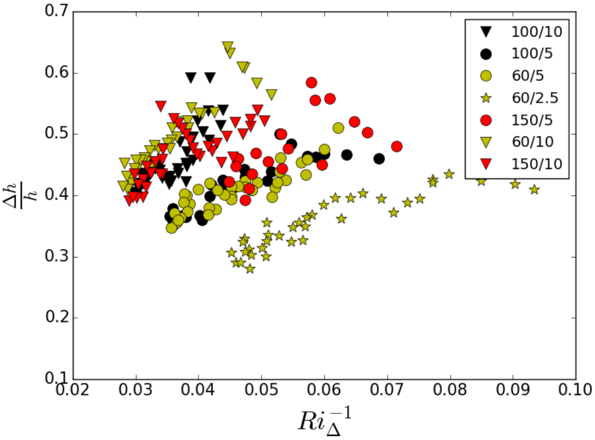

Figure 12: Plot of relationship of scaled EZ depth to Ri: $\frac{\Delta h}{h} \propto Ri^b$

Conclusion:

- **curves representing $\frac{\Delta h}{h} \propto Ri^b$ group according to γ when EZ is defined based on $\frac{\partial \bar{\theta}}{\partial z}$**

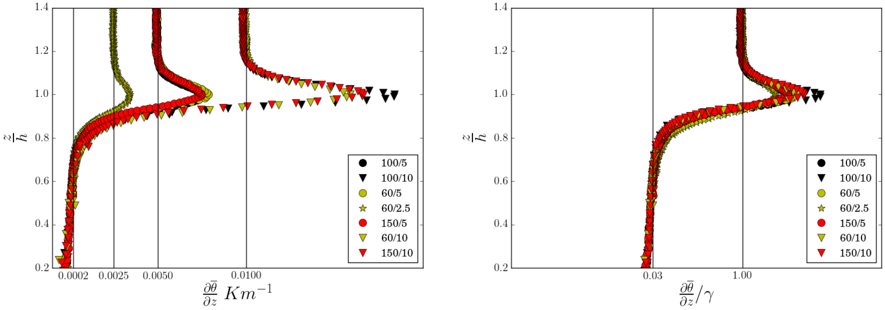

Figure 13: Definition of lower EZ boundary based on $\frac{\partial\overline{\theta}}{\partial z}$ (left) and $\frac{\partial\overline{\theta}}{\partial z}/\gamma$ (right)

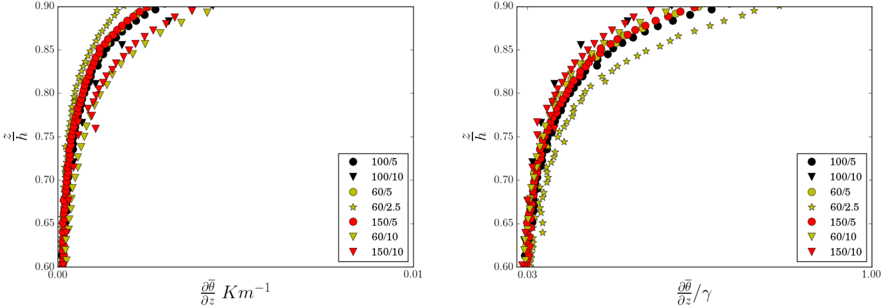

Figure 14: As previous slide, but zoomed in to show reversal in order of the magnitude of the lower EZ boundary.

:

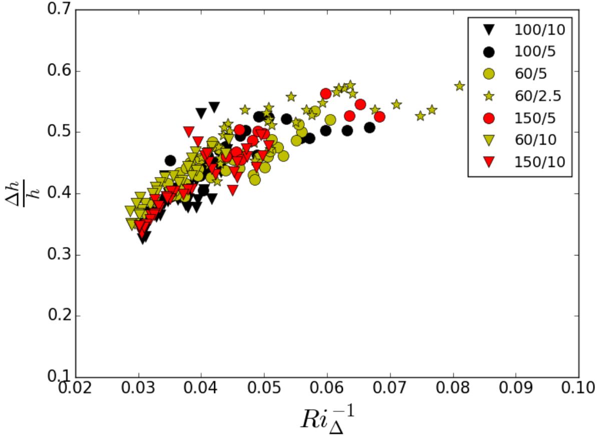

Figure 15: Plot of relationship of scaled EZ depth to Ri: $\frac{\Delta h}{h} \propto Ri^{b}$ with EZ boundaries based on $\frac{\partial \overline{\theta}}{\partial z}/\gamma$

Conclusion:

- **curves representing $\frac{\Delta h}{h} \propto Ri^{b}$ group according to γ when EZ is defined based on $\frac{\partial \overline{\theta}}{\partial z}$ but collapse when EZ is based on $\frac{\frac{\partial \overline{\theta}}{\partial z}}{\gamma}$**

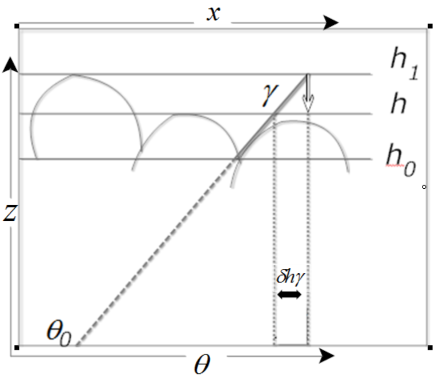

Figure 16: Representation of potential temperature fluctuation scale for the EZ $\delta h\gamma$

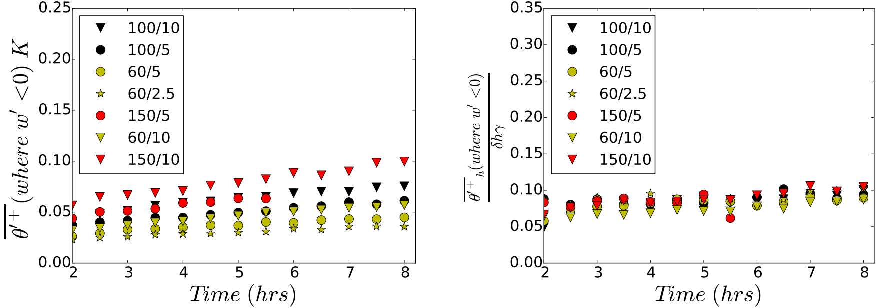

Figure 17: (left) Plot of the downward moving warm potential temperature fluctuation at h ($\overline{\theta'^+}_h$ where $w' < 0$). (right) $\overline{\theta'^+}_h$ where $w' < 0$ scaled by $\delta h\gamma$

Conclusion:

- **downward moving positive potential temperature fluctuations at** h **(**$\overline{\theta'^{+}}_{h}$ **where** $w^{'} < 0$**) are scaled by** $\delta h \gamma$

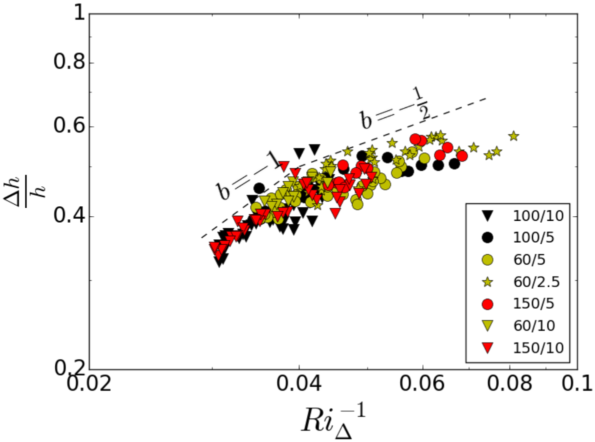

Figure 18: Plot of relationship of scaled EZ depth to *Ri*: $\frac{\Delta h}{h} \propto Ri^b$ with EZ boundaries based on $\frac{\partial \overline{\theta}}{\partial z}$*gamma* in log-log coordinates

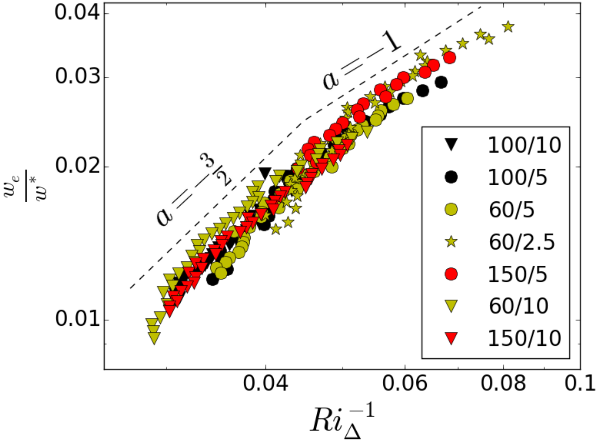

Figure 19: Plot of relationship of scaled CBL entrainment rate to Ri: $\frac{w_e}{w^*} \propto Ri^a$ with EZ boundaries based on $\frac{\partial \overline{\theta}}{\partial z}$*gamma* in log-log coordinates

Specific Conclusions:

- scaled EZ depth decreases with increased Ri
- $\overline{\theta'^{+}}_h$ where $w' < 0$ and $\frac{\partial \overline{\theta}}{\partial z}$ in the upper CBL depend on γ
- there is a change in entrainment regime with increased Ri
- definitions of CBL height and EZ boundaries based on the $\frac{\frac{\partial \overline{\theta}}{\partial z}}{\gamma}$ profile are valid

General Conclusions:

- given agreement with a recent DNS study SAM effectively models idealized CBL entrainment at this resolution
- Parametrizations f and entrainment zone thickness may need take regime change into consideration ie include a critical Ri

References

[1] Peter P. Sullivan and Edward G. Patton 2011: *The Effect of Mesh Resolution on Convective Boundary Layer Statistics and Structures Generated by Large Eddie Simulation*. Journal of the Atmospheric Sciences, 58, 2395-2415.

[2] Roland Stull 1988: *An Introduction to Boundary Layer Meteorology*. Kluwer Academic Publishers.

Thank You

especially to Douw, Phil and Roland :)

Questions?